

Half Semimetallic Antiferromagnetism in the Sr_2CrTO_6 System, $\mathcal{T} = \text{Os, Ru}$

K.-W. Lee^{1,2} and W. E. Pickett¹

¹ *Department of Physics, University of California, Davis, CA 95616, USA*

² *Department of Display and Semiconductor Physics, Korea University, Jochiwon, Chungnam-do 339-700, Korea*

(Dated: February 9, 2022)

Double perovskite $\text{Sr}_2\text{CrOsO}_6$ is (or is very close to) a realization of a spin-asymmetric semimetallic compensated ferrimagnet, according to first principles calculations. This type of near-half metallic antiferromagnet is an unusual occurrence, and more so in this compound because the zero gap is accidental rather than being symmetry determined. The large spin-orbit coupling (SOC) of osmium upsets the spin balance (no net spin moment without SOC): it reduces the Os spin moment by $0.27 \mu_B$ and induces an Os orbital moment of $0.17 \mu_B$ in the opposite direction. The effects combine (with small oxygen contributions) to give a net total moment of $0.54 \mu_B$ per cell in $\text{Sr}_2\text{CrOsO}_6$, reflecting a large impact of SOC in this compound. This value is in moderately good agreement with the measured saturation moment of $0.75 \mu_B$. The value of the net moment on the Os ion obtained from neutron diffraction ($0.73 \mu_B$ at low temperature) differs from the calculated value ($1.14 \mu_B$). Rather surprisingly, in isoivalent $\text{Sr}_2\text{CrRuO}_6$ the smaller SOC-induced spin changes and orbital moments (mostly on Ru) almost exactly cancel. This makes $\text{Sr}_2\text{CrRuO}_6$ a “half (semi)metallic antiferromagnet” (practically vanishing net total moment) even when SOC is included, with the metallic channel being a small-band-overlap semimetal. Fixed spin moment (FSM) calculations are presented for each compound, illustrating how they provide different information than in the case of a nonmagnetic material. These FSM results indicate that the Cr moment is an order of magnitude stiffer against longitudinal fluctuations than is the Os moment.

PACS numbers: 71.20.Be, 71.20.Dg, 71.55.Ak, 75.47.Np

I. INTRODUCTION

Precise compensation of magnetic moments in condensed matter systems, resulting in a vanishing total moment, occurs only in rare instances when not required by symmetry. One example is spin (S) and orbital (L) moment cancellation¹ in the Sm^{3+} (or any $4f^5$) ion, where Hund’s rule requires antialigned orientation of the spin and orbital moments ($M_z^S = 5\mu_B = -M_z^L$) along the quantization axis. Another example is so-called half metallic antiferromagnetism (HMAF), in which the integer spin moment in a half metal has the value zero.² Although not an AF (up and down spin directions are distinct), the up and down spin moments cancel exactly due to the half metallic nature. We will use the more precise term *compensated half metal* (CHM).³ Compensation in this case is no longer exact if spin-orbit coupling is not negligible.

After the initial description of the CHM concept,² a rational search for candidates was begun⁴ in the double perovskite (DP) family of oxides. DPs have been around for decades⁵ and new ones appear regularly. The suggestion that La_2MnVO_6 is a promising candidate has been pursued by Androulakis *et al.*,⁶ whose samples did not seem to assume the desired charge states but which also were not well ordered. The (full and half) Heusler structures have produced a number of HM ferromagnets,⁷ which have encouraged searches for a vanishing moment

member. Felser and collaborators identified a band-filling criterion for CHMs in Heusler materials, and were led to consider^{3,8} Mn_3Ga , which is calculated to be very near being a CHM (there is slight band overlap). In this compound two Mn $S = 1$ moments compensate one Mn $S = 2$ moment. Recently in the DP class, Park and Min⁹ have calculated possible CHMs in the quintinary $\text{La}_4\text{AVMoO}_6$ system, $\mathcal{A} = \text{Ca, Sr, Ba}$, which are as yet unsynthesized. Nakao has extended the search for CHMs to tetrahedrally coordinated transition metal based chalcopyrites.¹⁰ A true CHM is not yet a laboratory reality.

Originally reported 35 years ago by Sleight and coworkers,¹¹ the compound $\text{Sr}_2\text{CrOsO}_6$ (SCOO) has been revisited by Kronkenberger *et al.*¹² The motivation was that this member follows a series of (known or suspected) half metals Sr_2CrTO_6 , $\mathcal{T} = \text{W, Re}$, with very high magnetic ordering temperatures ($T_N \sim 500$ K and 635 K, respectively). SCOO has an even higher ordering temperature $T_N = 725$ K, the highest known in this class, and was reported to be insulating. The Cr^{3+} and Os^{5+} ions both have a filled majority t_{2g} subshell and high spin $S = 3/2$, eliminating possible complications due to orbital fluctuations and orbital ordering and making it straightforward to address the electronic and magnetic structure. The calculated densities of states (DOS) indicate¹² that, before Spin-orbit coupling (SOC) is included, the system is compensated ferrimagnet with a very small gap. The structure is cubic

above ~ 500 K, but distorts slightly below that temperature to rhombohedral $R\bar{3}$ symmetry, consistent with the magnetic symmetry.

In this paper we look in more detail at the electronic structure of SCO, which also prompts us to check the isovalent material $\text{Sr}_2\text{CrRuO}_6$ (SCRO). First principles calculations, of the same sort that predict Sr_2CrWO_6 and $\text{Sr}_2\text{CrReO}_6$ to be HMs, predict that SCO is (before considering SOC) actually a ferrimagnetic semimetal with precisely compensating spin moments, or *spin-asymmetric compensated semimetallic ferrimagnet* in which the electrons and the holes are each fully polarized and have *opposite* spin directions, in spite of zero net moment and hence no macroscopic magnetic field. This is a peculiar state indeed. SOC degrades this by giving a nonzero total moment, but the band structure is little changed. We then look at the isovalent system SCRO, and find that due to small but important chemical differences, it is also a *compensated half (semi)metal* and moreover the total (spin + orbital) moment remains vanishingly small. This is a CHM in which the metallic channel is semimetallic rather than fully metallic, with the semimetallic channel having spin in the direction of the Cr spin (the Ru spin is antialigned).

II. THEORETICAL AND COMPUTATIONAL METHODS

Our calculations are based on both cubic (500 K) and rhombohedral ($R\bar{3}$, at 2 K) structures.¹² In the distorted structure, the change in volume is less than 1%, and O and Sr atoms are displaced by 0.015 and 0.006 Å, respectively. Since comparison between perovskite SrOsO_3 ¹³ and SrRuO_3 ¹⁴ shows about 1% volume difference, difference in structures between SCRO and SCO is expected to be negligible. Calculations (as described below) are consistent, obtaining a 1% smaller lattice constant for $\text{Sr}_2\text{CrRuO}_6$ (7.62 Å) than for $\text{Sr}_2\text{CrOsO}_6$ (7.706 Å). Since we wish here to interpret the experimental electronic properties as closely as possible, we use for our calculations the same experimental structures of SCO (also used for SCRO). These are the values $a=7.8243$ Å for the cubic, and $a=5.5176$ Å, $c=13.445$ Å for the rhombohedral structures.¹²

These calculations were carried out with the local spin density approximation (LSDA) and spin-orbital coupling (SOC) or fully relativistic scheme¹⁵ implemented in two all-electron full-potential codes, FPLO¹⁶ and Wien2k¹⁷, which showed consistent results. In FPLO, basis orbitals were chosen such as Os ($4f5s5p$) $6s6p5d$, Ru ($4s4p$) $5s5p4d$, Cr ($3s3p$) $4s4p3d$, Sr ($4s4p$) $5s5p4d$, and O $2s2p3d$.

(The orbitals in parentheses indicate semicore orbitals.) In Wien2k, the basis size was determined by $R_{mt}K_{max}=7.0$ and APW sphere radii (1.95 for Os/Ru, 1.94 for Cr, 2.47 for Sr, and 1.72 for O). Although the semimetallic character does not require a lot k -points like a metal would, the Brillouin zone was sampled carefully with (20,20,20) k -mesh. A carefully k -mesh sampling is necessary for SOC and fixed spin moment (FSM) calculations. The FSM calculations we describe were done with the FPLO code.

For SCO we find the $R\bar{3}$ distortion is energetically favored, in agreement with observation. We also find that SCRO in the $R\bar{3}$ structure is favored over the cubic structure, by 145 meV. The distortions (apparently due to size mismatch) in either compound have negligible affect on the electronic structure, consistent with the fact that both ions have a filled t_{2g} shell so that band structure energy is not gained by the distortion.

III. RESULTS AND INTERPRETATION

A. LSDA electronic structure of SCO

The LSDA band structure near E_F (without SOC) of SCO, which has antialigned $S = \frac{3}{2}$ moments on both Cr and Os and hence zero net moment, is shown in Fig. 1 and agrees with that of Krockenberger *et al.*¹² The fully occupied Os (‘down’, by our choice) and Cr (up) majority t_{2g} manifolds each have identical width of 1.8 eV, shifted by 0.3 eV in energy. The lowest spin-up conduction band at L is degenerate with the filled Os t_{2g} band maximum (flat along X-W), defining E_F at the point of (accidentally occurring) zero gap. The larger transition metal-O hybridization for a 5d ion compared to that of a 3d ion reduces the Os spin moment from 3 μ_B by almost a factor of two, even though both Cr and Os ions have occupied t_{2g} states corresponding to $S = 3/2$.

Now we will focus on results of the SCO zero temperature $R\bar{3}$ structure. As shown in Table I, the Cr spin moment of 2.2 μ_B is completely compensated with the Os spin moment of $-1.6 \mu_B$ and the six O moments. As displayed in the corresponding DOS given in the top panel of Fig. 2, each spin channel separately has a gap, 0.4 eV for the spin-up and 1 eV for spin-down, between the Cr and Os t_{2g} manifolds. The majority and minority states show different hybridization, resulting in differing crystal (ligand) field and exchange splittings on Cr and Os. The crystal field splittings Δ_{cf} are (roughly): Cr, majority 2.5 eV, minority 1 eV; Os: 2.5-3 eV for both directions. The exchange splitting in the Os

TABLE I: LSDA and LSDA+SOC results for individual and total spin M_S , orbital M_L , and net M_{net} moments (μ_B) in the $R\bar{3}$ structure. The effect of SOC is primarily on the Os ion, and changes the magnetic character considerably in $\text{Sr}_2\text{CrOsO}_6$ but little in $\text{Sr}_2\text{CrRuO}_6$.

Compound	LSDA			LSDA+SOC						
	Cr	Os/Ru	M_S	Spin			Orbital			
				Cr	Os/Ru	M_S	Cr	Os/Ru	M_L	M_{net}
$\text{Sr}_2\text{CrOsO}_6$	2.22	-1.58	0.00	2.194	-1.312	0.399	-0.025	0.173	0.142	0.541
$\text{Sr}_2\text{CrRuO}_6$	2.08	-1.48	0.00	2.079	-1.474	0.025	-0.048	0.031	-0.020	-0.005

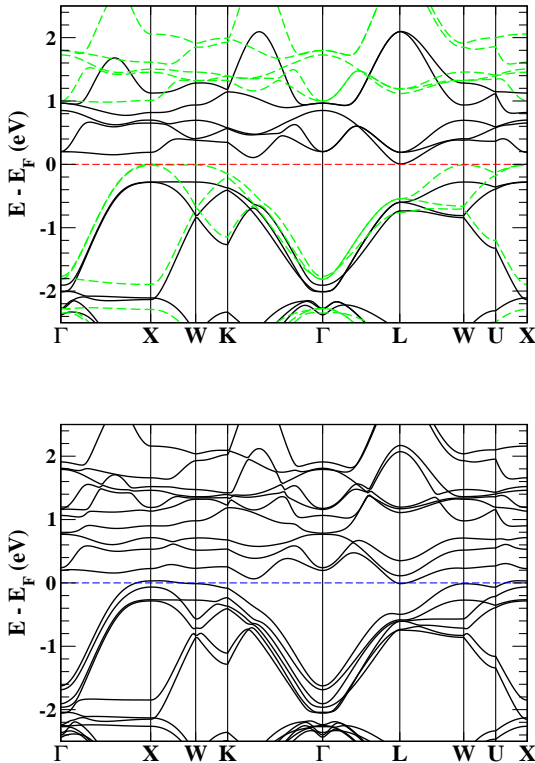


FIG. 1: (color online) Top panel: LSDA band structure $\text{Sr}_2\text{CrOsO}_6$, excluding spin-orbit coupling, in the distorted $R\bar{3}$ structure for each spin channel (dashed and solid lines for the majority and minority channels, respectively). This plot contains the Cr d bands and Os t_{2g} manifold. The O p bands lie in the range -8.5 to -2 eV, and the Os e_g manifold lies above 4 eV due to large crystal field splitting. Note the flat bands along the $X - W$ lines near E_F , which lead to a quasi-two-dimensional DOS at either spin channel (see Fig. 2). The symmetry labels follow the conventional fcc notation. The horizontal dashed line indicates the Fermi energy E_F set to zero. Bottom panel: The band structure of $\text{Sr}_2\text{CrOsO}_6$ with spin-orbit coupling included. The slightly negative gap is due to small overlap of the conduction at L with the upper valence band at X. The optical gap is ~ 0.25 eV.

ion (just over 1 eV) is half of that of Cr ion.

The distinguishing feature of SCO is that the Os t_{2g} bandwidth is equal to its exchange splitting, such that the zero gap lies ‘between’ the corresponding up and down bands. Upon including SOC, the Cr moment (with its small SOC) is almost unchanged. The effect on Os is substantial, however; due to mixing with states of the opposite spin, the spin moment is reduced by $0.27 \mu_B$ and an orbital moment of $-0.17 \mu_B$ is induced. The total net moment, $0.54 \mu_B$ reflecting both spin and orbital compensation, is reasonable close to the observed value¹² of $0.75 \mu_B$. (The unusual temperature dependence indicates non-standard behavior of the magnetism in SCO, so it may be premature to expect close agreement.) The total DOS, given in the inset of the top panel in Fig. 2, indicates filling of the up-spin gap due to Os spin-mixing.

Krockenberger *et al.*¹² have reported moments of $\text{Sr}_2\text{CrOsO}_6$ obtained from neutron scattering, which are net (spin+orbital) values for Os and Cr. These moments should not be expected to be identical to the calculated values, both because the theoretical specification involves an assignment of the spin density using inscribed atomic spheres (and some spin polarization in the interstitial region not assigned to either), and because the neutron fitting takes no account of the difference of spin and orbital form factors. The experimental values are $M = 2.03$ (-0.73) μ_B for Cr (Os). Our calculated values are $M = 2.17$ (-1.14) μ_B , respectively, which are close to those calculated earlier.¹² The difference for the Os ion (which amounts to about +25% and -25% from the mean of $-0.95\mu_B$) is large enough to be bothersome, and should be the object of further study. It has recently been observed that the net moment on Os^{7+} in $\text{Ba}_2\text{NaOsO}_6$ is affected very peculiarly¹⁸ by the large SOC on Os, and although the Os^{5+} ion will differ substantially, the orbital component will need to be taken into account explicitly to clarify this discrepancy.

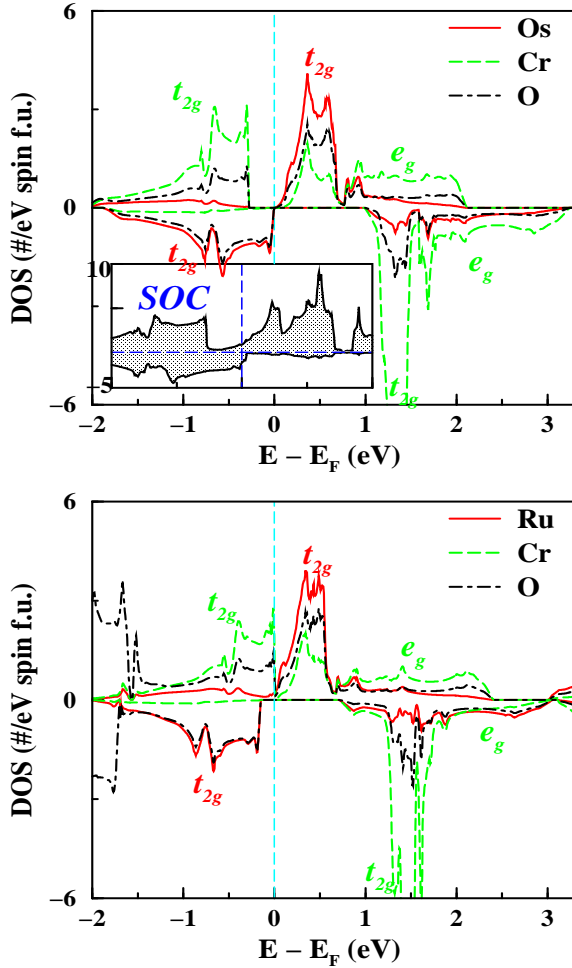


FIG. 2: (color online) Top panel: LSDA (without SOC) atom-projected densities of states (DOS) per a formula unit for each spin channel of $\text{Sr}_2\text{CrOsO}_6$ in the distorted structure. The occupied Os t_{2g} manifold has 50% O character in the whole range, while in the occupied Cr t_{2g} manifold O contributes less than half of Cr contribution to DOS. The vertical dashed line denotes E_F . Inset: LSDA+SOC total DOS (in the same units as above) in the range of 1 eV above and below E_F , where SOC effects are dominant, indicated by the vertical dashed line. The horizontal dashed line represents zero DOS. Bottom panel: similar plot for $\text{Sr}_2\text{CrRuO}_6$ in the distorted structure. The O p bands locate at the range -7.5 eV to -1.5 eV (not shown here). Unlike for SCOO, the DOS of SCRO is hardly affected by SOC.

B. The Ru analog $\text{Sr}_2\text{CrRuO}_6$

SCRO shows some distinctions from SCOO, small but sufficient to change the character of the spectrum. Both Cr and Ru moments are 7-9% smaller than in SCOO, but the system is still representative of compensating $S = \frac{3}{2}$ moments with vanishing net

spin. Relative to the Ru (minority) bandwidth, the Ru exchange splitting is larger, and the on-site energy on Ru is enough lower to alter the distinguishing features of the states at low energy. The result is that E_F is pinned in a ‘zero gap’ between the occupied Cr t_{2g} bands and unoccupied Ru t_{2g} bands (there is actually a slight ~ 0.1 eV band overlap).

A crucial difference from SCOO is that the zero total moment of SCRO (due to half metallicity) survives SOC: the slight net spin moment of $0.025 \mu_B$ is compensated by the induced orbital moment of $-0.020 \mu_B$, see Table I. This size of moment is negligible compared to other uncertainties, and we conclude that SCRO remains effectively half metallic in the presence of SOC.

C. Metal versus insulator question

To address the reported insulating character in SCOO (versus the low DOS semimetal result obtained above), we applied intra-atomic Coulomb repulsion U on Os (or Ru in SCRO) ion using LDA+ U method^{19,20} implemented in FPLO.²¹ As expected beginning from the zero gap in SCOO, for U as small as 0.5 eV an insulating phase is obtained. Across the metal-insulator transition and into the insulating phase, the compensated moment in both SCOO and SCRO remains unchanged for all U . Here the opening of the gap is not such as to produce a Mott insulator (it is a band insulator), but rather in the mold of a ‘energy gap correction’ to LSDA, which might better be accomplished by self-energy corrections suitable for itinerant state (if it is needed at all).

An important implication is that the Os $5d$ electrons in SCOO are not in localized, strongly correlated states but closer to itinerant. If this is the case, pressure will more readily produce metalization and lead to a CHM (degraded by SOC). Calculations confirm that the main effects of pressure are to increase bandwidths, thereby reducing the moments and the associated exchange splittings and generally increasing itineracy. The differences displayed by SCRO relative to SCOO suggest that it may not be insulating even at ambient pressure, in which it provides the first example of a CHM, not even blemished noticeably by SOC. The strong hybridization of the Os and Ru d states, which is the cause of itineracy, is evident in the moment that opposes that of Cr: it is $\sim 1.4 \mu_B$ on the metal, and $0.7 \mu_B$ distributed over the neighboring O ions (Table I). This strong \mathcal{T} - d -O $2p$ mixing, together with the robust $S = \frac{3}{2}$ moments, is almost certainly at the root of the remarkably high magnetic ordering temperature of 750 K.

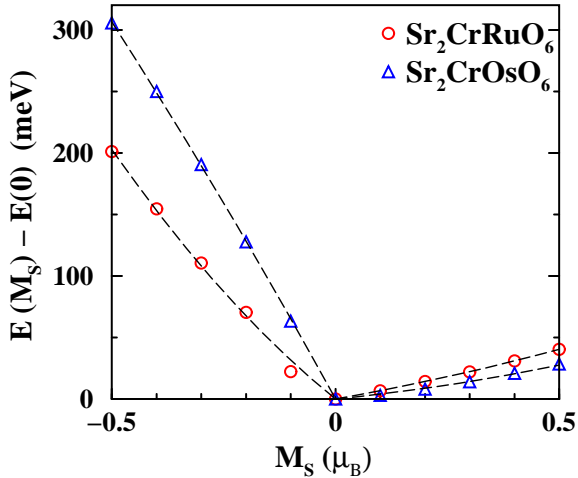


FIG. 3: (color online) LSDA fixed spin moment M_S calculations. Since the minority channels have much larger gap in both systems, the plots are highly asymmetric with respect to the ground state occurring at $M_S = 0$. The dashed lines indicate fitting curves using a formula $E(M_S) - E(0) = aM + bM^2$.

D. Fixed Spin Moment Studies

In a conventional, unpolarized metal fixed spin moment (FSM) calculations^{22,23} provide at small M the (interaction enhanced) susceptibility $\delta E(M) = \frac{1}{2}\chi^{-1}M^2 + \dots$, and gives the Stoner instability if the energy *decreases* with moment M . At larger M stable or metastable magnetic states may be uncovered. The behavior is quite different in a half metal, where the spin densities (and the ground state itself) are invariant to any applied magnetic field that does not cause the Fermi level in the metallic channel to cross a band edge of the insulating channel.²⁴ Once the crossing occurs, one can again carry out FSM calculations to analyze the $E(M)$ relation and the differential susceptibility. While $E(M)$ is analytic (and even in M) in a nonmagnetic metal, in a HM $E(M)$ is non-analytic at $M=0$ and is asymmetric, and may be strongly asymmetric. The point single $M=0$ (in SCOO, since it is spin compensated) corresponds to a huge range of magnetic field $\Delta B = E_{gap}/\mu_B$.

We choose the Cr moment direction to define ‘up’ in the following discussion, hence a positive field is parallel to the Cr moment. At zero field the net moment is zero, and positive and negative fields do not change the moment until they become large enough to shift the Fermi level across a ‘down’ spin band edge. At the onset of change in the moment the behavior in a HM differs from that of conventional FSM behavior because of the strong density of states

variation

$$N(E) \propto m^* \sqrt{|E - E_o|} \quad (1)$$

at the band edge, where m^* is the effective mass. As a result the differential susceptibility $-d^2\mathcal{E}/d^2H$ at the edge is non-analytic in M . In SCOO, however, the top of the occupied Cr t_{2g} bands display essentially two-dimensional step-function behavior shown in Fig. 2, top panel, (not uncommon in perovskite structures), and beyond the onset the DOS varies slowly. The form of the differential susceptibility at the conduction band edge (positive moment) is

$$\chi(M) = -d^2\mathcal{E}/d^2H \propto \alpha + \gamma m^* \sqrt{M}, \quad (2)$$

where α, γ are material-dependent constants. The calculated FSM $E(M)$ curves for both compounds are displayed in Fig. 3. The non-analytic behavior is confined to low moment ($M \approx 0$) and is not clear on this scale.

The strong asymmetry is striking. For positive applied field, the up spin states in Fig. 2 move down with respect to the down states. Because the exchange splitting is much smaller on Os than on Cr, the moment on Os decreases (transfer of electrons from Os t_{2g} down to Os t_{2g} up) and the energy cost is relatively small, see Fig. 3 for positive M_s . For negative applied field, the relative shift of states is in the opposite direction, and the shift in filled states is from Cr t_{2g} up to Cr t_{2g} down, and this field direction decreases the Cr moment. The energy cost of changing the Cr moment is roughly an order of magnitude larger than for Os: the Os moment is much ‘softer’ than is that of Cr. Interestingly, the Cr moment softens by one-third in SCRO, due to differences in hybridization, and the Ru moment is somewhat stiffer than the Os moment.

IV. DISCUSSION

We have applied first principles, full potential, all-electron methods to assess the electronic and magnetic structures of $\text{Sr}_2\text{CrOsO}_6$ and $\text{Sr}_2\text{CrRuO}_6$. We have shown that the observed saturation moment of ferrimagnetic $\text{Sr}_2\text{CrOsO}_6$ is entirely due to spin-orbit coupling, and without this coupling $\text{Sr}_2\text{CrOsO}_6$ would be spin-compensated (zero net moment). We have also studied isostructural, isovalent $\text{Sr}_2\text{CrRuO}_6$, which has not yet been synthesized in ordered form. Due to the much smaller spin-orbit coupling in Ru, this compound remains a spin-compensated ferrimagnetic (to within $0.02 \mu_B$), and therefore is a realization of a half (semi)metallic antiferromagnet.

We have also investigated the other isovalent partner $\text{Sr}_2\text{CrFeO}_6$ using the same structures as for

SCOO. The smaller hybridization of Fe increases the spin moment to $3 \mu_B$, and the Cr moment decreases ($1.3 \mu_B$). The result is a simple metallic ferrimagnet with a net spin moment of $2.25 \mu_B$.

Williams *et al.* reported Cr-Ru disorder²⁵ in their study of the $\text{SrCr}_{1-x}\text{Ru}_x\text{O}_3$ system. However, the negligible difference of 0.01 \AA in the Ru^{5+} and Os^{5+} ionic radii²⁶ and the identical charge state suggest that ordered SCRO would result from the high temperature technique that produces (almost perfectly) ordered SCOO.¹² Another approach would proceed by alternating Cr and Ru deposition in layer-by-layer epitaxy, either molecular beam epitaxy or pulsed laser deposition, a process which produces the double perovskite structure for $\langle 111 \rangle$ growth. Thus prospects should be good for checking for the CHM state (“half metallic antiferromagnetism”) in $\text{Sr}_2\text{CrRuO}_6$.

Finally, we have performed the first (to our knowledge) extension of the fixed spin moment technique

to a half metallic compound. We describe how this technique provides different and still important information for a half metal. For $\text{Sr}_2\text{CrOsO}_6$, it indicates that longitudinal fluctuation in the magnetic moment of Os in $\text{Sr}_2\text{CrOsO}_6$ is about ten times as large as for the Cr moment. In $\text{Sr}_2\text{CrRuO}_6$, this dissimilarity is reduced to about a factor of five.

V. ACKNOWLEDGMENTS

We acknowledge clarification of the crystal structure by M. Reehuis and M. Jansen, communication with W. H. Butler on fixed spin moment calculations in half metals, and discussions with C. Felser on these compounds. This work was supported by DOE grant DE-FG03-01ER45876, and interaction within DOE’s Computational Materials Science Network is acknowledged.

-
- ¹ H. Adachi, H. Kawata, H. Hashimoto, Y. Sato, I. Matsumoto, and Y. Tanaka, *Phys. Rev. Lett.* **87**, 127202 (2001).
- ² H. van Leuken and R. A. de Groot, *Phys. Rev. Lett.* **74**, 1171 (1995).
- ³ S. Wurmehl, H. C. Kandpal, G. H. Fecher, and C. Felser, *J. Phys.: Condens. Matter.* **18**, 6171 (2006).
- ⁴ W. E. Pickett, *Phys. Rev. B* **57**, 10613 (1997).
- ⁵ K. R. Poeppelmeier, *Prog. Solid State Chem.* **22**, 197 (1993).
- ⁶ J. Androulakis, N. Katsarakis, and J. Giapintzakis, *Solid State Commun.* **124**, 77 (2002).
- ⁷ W. E. Pickett and J. S. Moodera, *Physics Today* **54**, 39 (2001) and references therein.
- ⁸ B. Balke, G. H. Fecher, J. Winterlik, and C. Felser, *Appl. Phys. Lett.* **90**, 152504 (2007).
- ⁹ M. S. Park and B. I. Min, *Phys. Rev. B* **71**, 052405 (2005).
- ¹⁰ M. Nakao, *Phys. Rev. B* **74**, 172404 (2006).
- ¹¹ A. W. Sleight, J. Longo, and R. Ward, *Inorg. Chem.* **1**, 245 (1962).
- ¹² Y. Kronenberger, K. Mogare, M. Reehuis, M. Tovar, M. Jansen, G. Vaitheeswaran, V. Kanchana, F. Bultmark, A. Delin, F. Wilhelm, A. Winkler, and L. Alff, *Phys. Rev. B* **75**, 020404(R) (2007).
- ¹³ B. L. Chamberland, *Mat. Res. Bull.* **13**, 1273 (1978).
- ¹⁴ K. Maiti, *Phys. Rev. B* **73**, 235110 (2006), and references therein.
- ¹⁵ H. Eschrig, M. Richter, and I. Opahle, in *Relativistic Electronic Structure Theory—Part II*, edited by P. Schwerdtfeger (Elsevier, Amsterdam, 2004), pp. 723-776.
- ¹⁶ K. Koepnik and H. Eschrig, *Phys. Rev. B* **59**, 1743 (1999).
- ¹⁷ P. Blaha, K. Schwarz, G. K. H. Madsen, D. Kvasnicka, and J. Luitz, *Wien2k, An Augmented Plane Wave and Local Orbitals Program for Calculating Crystal Properties* (Karlheinz Schwarz, Technical Universität Wien, Wien 2001), ISBN 3-950/031-1-2.
- ¹⁸ K. W. Lee and W. E. Pickett, *Europhys. Lett.* **80**, 37008 (2007).
- ¹⁹ V. I. Anisimov, I. V. Solovyev, M. A. Korotin, M. T. Czyzyk, and G. A. Sawatzky, *Phys. Rev. B* **48**, 16929 (1993).
- ²⁰ M. T. Czyzyk and G. A. Sawatzky, *Phys. Rev. B* **49**, 14211 (1994).
- ²¹ H. Eschrig, K. Koepnik, and I. Chaplygin, *J. Solid State Chem.* **176**, 482 (2003).
- ²² O. K. Andersen, J. Madsen, U. K. Paulsen, O. Jepsen, and J. Kollar, *Physica B* **86-88**, 249 (1977).
- ²³ G. L. Krasko, *Phys. Rev. B* **36**, 8565 (1987).
- ²⁴ H. Eschrig and W. E. Pickett, *Solid State Commun.* **118**, 123 (2001).
- ²⁵ A. J. Williams, A. Gillies, J. P. Attfield, G. Heymann, H. Huppertz, M. J. Matínez-Lope, and J. A. Alonso, *Phys. Rev. B* **73**, 104409 (2006).
- ²⁶ <http://www.webelements.com/>